

Appendix P—Models of Earthquake Recurrence and Down-Dip Edge of Rupture for the Cascadia Subduction Zone

By Arthur D. Frankel,¹ and Mark D. Petersen¹

Introduction

Logic trees for the recurrence of great earthquakes on the Cascadia Subduction Zone (CSZ) were developed from discussions at the November 2010 and March 2012 workshops, which were held for the purpose of updating the U.S. national seismic hazard maps (NSHM) and for the Uniform California Earthquake Rupture Forecast, Version 3 (UCERF3). The location of the down-dip edge of the rupture zones of CSZ great earthquakes was debated during workshops in December of 2011 and March of 2012. A logic tree for the position of the down-dip edge was also developed from these deliberations.

Logic Trees for CSZ Recurrence

The November 2010 workshop focused on evaluating the analysis and interpretation of turbidites in deep-ocean cores by Goldfinger and others (2012) to constrain the recurrence time and magnitudes of great earthquakes on the CSZ. This workshop is summarized in Frankel (2011). Figure P1 from Goldfinger and others (2012) shows the great earthquake rupture zones that they estimated from the 10,000-year turbidite record. The key result of the 2010 workshop was that the participants accepted the idea of *M*8 earthquakes that rupture only the southern part of the CSZ. Evidence for these earthquakes is manifested in turbidites (Goldfinger and others, 2008, 2012) and in tsunami deposits found on land at Sixes River (Kelsey and others, 2002) and Bradley Lake (Kelsey and others, 2005; Nelson and others, 2006) in southwestern Oregon. The participants workshop also heard evidence presented by Brian Atwater on the possibility of *M*8 earthquakes that only rupture the northern portion of the CSZ, mainly inferred from tsunami deposits at Discovery Bay reported by Williams and others (2005).

These partial CSZ rupture earthquakes supplement the whole CSZ ruptures with moment magnitudes inferred to be about 9.0, based on observations and modeling of the tsunami in Japan that was likely generated by the 1700 Cascadia earthquake (Satake and others, 1996, 2003). These whole CSZ rupture earthquakes have been well documented from about 5,000 years of evidence of coastal subsidence, tsunami deposits, and liquefaction at numerous sites near the coast in Washington, Oregon, and northern California

¹U.S. Geological Survey.

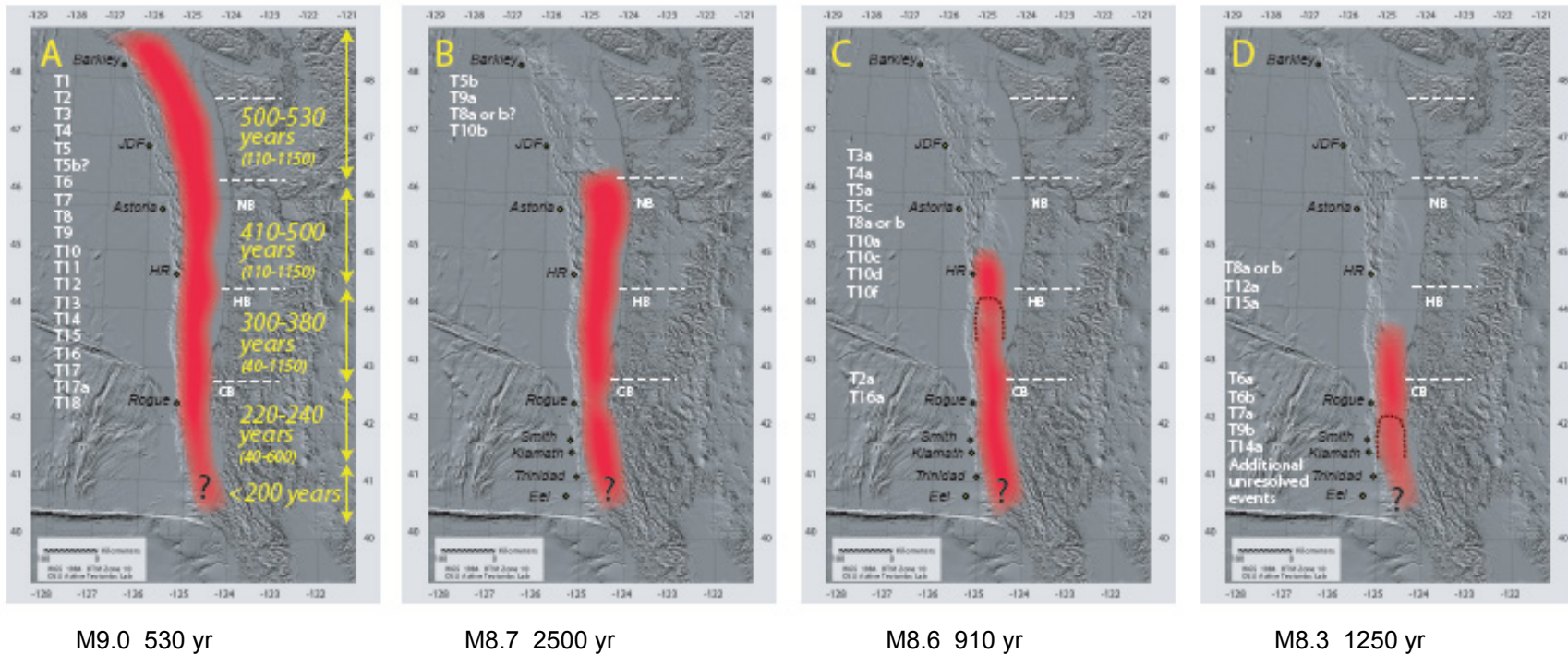


Figure P1. Four-panel figure taken from Goldfinger and others (2012) showing rupture zones of great Cascadia earthquakes that they determined from the turbidite record over the past 10,000 yr. Black dots are locations of cores. Designation of great earthquakes for each rupture scenario are shown on left side of each panel (for example, T1, T5b). CB= Cape Blanco. HB = Heceta Bank. NB = Nehalem Bank. Below each panel, we added the preferred magnitude and recurrence time used for each rupture scenario in our initial implementation of the Goldfinger and others (2012) rupture model. Recurrence times determined by dividing 10,000 yr by the number of earthquakes in that scenario.

(for example, Atwater, 1987, 1992; Atwater and Hemphill-Haley, 1997; Nelson and others, 1996; Kelsey and others, 2002, 2005; Witter and others, 2003), as well as from 7,500–10,000 years of turbidites (Adams, 1990; Goldfinger and others, 2003, 2008). Workshop participants agreed that a mean recurrence time of about 500–550 years was appropriate for these whole CSZ ruptures, with an important caveat. They also thought that some of these 500–550 year scenarios may have been a series of *M*8 earthquakes that ruptured the whole CSZ over several years or a couple of decades, similar to what has been observed for the Nankai Trough in Japan (1944 and 1946) and along the Columbia-Ecuador coast of South America (1942–1979).

The participants of the November 2010 workshop also came to a consensus that the next NSHM and UCERF3 should use a mean recurrence rate of 0.001 per year for *M*8 earthquakes that only rupture the southern part of the CSZ. This rate is about half the rate for these earthquakes that was determined by Goldfinger and others (2012). One motivation for this choice was that this rate of partial CSZ ruptures is similar to that observed over certain periods of time at Sixes River and Bradley Lake. This mean-recurrence rate is viewed by some workshop participants as a compromise position, pending future research. As new work on the turbidites and other evidence is accomplished, the mean rate for the hazard maps should be reassessed. No consensus on the rate of partial CSZ ruptures in the northern CSZ was reached at the November 2010 workshop.

Figure P2 shows the two proposed logic trees for CSZ recurrence. The hazard (frequency of exceeding a specified ground motion) from these two logic trees is additive. For the whole rupture of the CSZ (fig. p2, bottom), we consider aleatory uncertainty by having *M*8.6–9.3 earthquakes that rupture the whole CSZ (80% of sequences) and the possibility of serial *M*8 earthquakes that rupture the entire CSZ over a period of a few decades or less (20% of sequences). The average recurrence time is 530 years, either for the whole-rupture earthquakes or the series of *M*8 earthquakes.

The lower probability (20% of the sequences) for the serial *M*8 rupture reflects a number of factors. Having an *M*8 earthquake rupture at any location every 500 years, as part of a rupture sequence, would obviously produce less slip than an *M*9 earthquake rupturing the whole zone every 500 years. The overall plate motion of about 40 mm/yr can be accommodated with *M*9 earthquakes occurring every 500 years with an average slip of 20 m per event. This plate rate cannot be accommodated by *M*8.3–8.5 earthquakes with a 500-year-recurrence time at any particular rupture location. This would be a problem if the shallow (< 30 km depth) part of the subduction interface were highly coupled. Bird and Kagan (2004) found a high coupling factor for a global collection of subduction zones, using a Gutenberg-Richter (GR) recurrence model with parameters derived from the observed seismicity. However, it does not appear that earthquakes on the Cascadia subduction zone follow a Gutenberg-Richter distribution, given the lack of historically observed earthquakes with magnitudes less than 7 on most of the zone. Pacheco and others (1993) found low coupling factors in many subduction zones, although their results were based on only a 90-year catalog of seismicity. Goldfinger and others (2012) do not see evidence of *M*8 serial ruptures in the Cascadia turbidite data. A time-independent hazard calculation for the serial ruptures could be done using the procedure in Toro and Silva (2001), similar to the approach used in the 2008 NSHMs for clustering of 1811–12 type New Madrid earthquakes (Petersen and others, 2008).

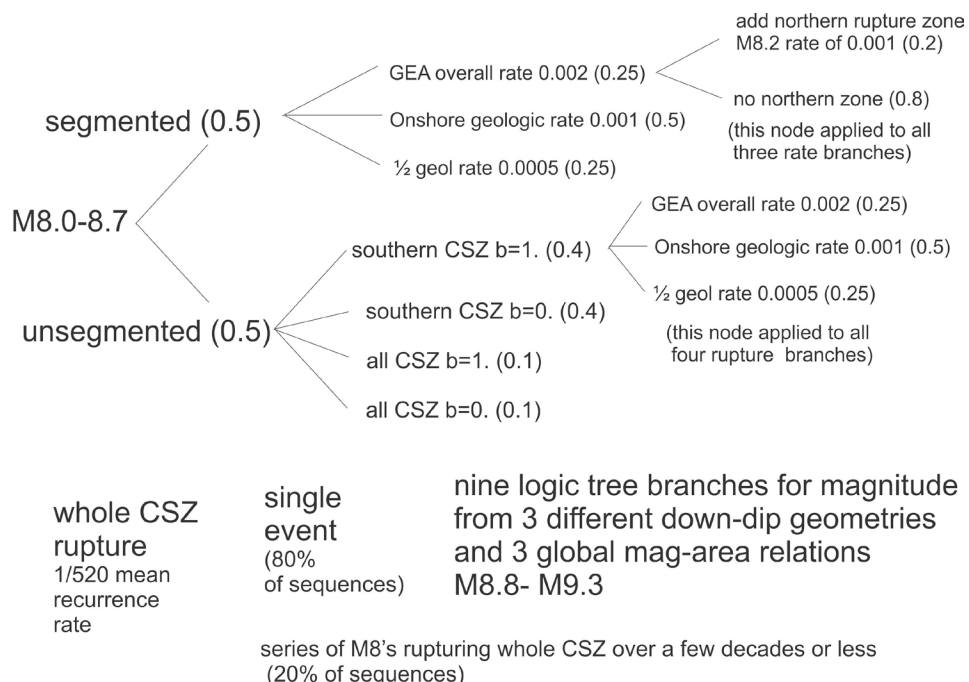


Figure P2. Proposed logic trees for recurrence of great Cascadia earthquakes. Note that the hazard (frequency of exceeding any given ground motion) from whole Cascadia Subduction Zone (CSZ) ruptures and partial ruptures with M8.0–8.7 is additive. Initial weight for each branch is given in parentheses. GEA denotes the Goldfinger and others (2012, fig. 1) rupture rate.

To determine the magnitudes of the whole and partial CSZ ruptures we first calculate the rupture area using a logic tree involving the three down-dip edges of rupture described below. Then we use a logic tree consisting of three global magnitude area relations developed for subduction zone interface earthquakes: Papazachos and others (2004), Murotani and others (2008), and Strasser and others (2010). So for each rupture scenario there are nine different values of magnitude used in the logic tree, each with equal weight. For the whole CSZ ruptures, the magnitudes range from 8.6 to 9.3. Rui Chen of the California Geological Survey calculated the rupture areas and magnitudes used in the draft update of the national seismic hazard maps.

The logic tree shown at the top of figure P2 characterizes the hazard from individual earthquakes with magnitudes between 8.0 and 8.7 that rupture only a part of the CSZ. The first node of the M8.0–8.7 logic tree is for segmented versus unsegmented rupture models, which are given equal weight. Goldfinger and others (2012) presented a rupture model with rupture boundaries chosen at Cape Blanco, Heceta Bank, and Nehalem Bank, approximately (fig. P1). This model is used in the “segmented” branch of the logic tree. Participants in the November 2010 workshop thought that Cape Blanco represented a likely segment boundary, for multiple reasons. The age of the incoming subducting plate varies from north to south at this location. While there is a marked difference in age for the incoming plate at the trench at this latitude, Wilson (2002) finds that the age difference is less pronounced in the portion of the plate beneath the coast (P. McCrory, written commun., 2013). Cape Blanco is also near the latitude of the southern edge of the mafic Siletz block on the overriding plate (Burgette and others, 2009). There is more disagreement on whether Heceta Bank and Nehalem Bank represent possible

segment boundaries. The turbidite data are from a limited number of coring sites and can be interpreted with either segmented or unsegmented rupture models.

An earlier version of these logic trees was described and discussed at the March 21–22, 2012, workshop for the update of the Pacific Northwest part of the U.S. national seismic hazard maps. Some participants suggested that a more formal treatment of the logic tree describing the rate for partial CSZ ruptures ($M8.0-8.7$) should be used. This rate has been adopted in the revised logic tree in figure P2. The consensus rate of 0.001 per year for southern CSZ $M8$ events was still advocated by most of the people who expressed an opinion at the March 2012 workshop.

For the logic tree node representing the overall recurrence rate of southern ruptures, we use three branches: (1) The rate from onshore geologic observations (about 0.001 per year), (2) the rate from Goldfinger and others (2012; about 0.002 per year), and (3) a rate of 0.0005 per year reflecting the possibility that some of the onshore and offshore observations may not reflect great earthquakes on the CSZ and also recognizing that there are periods of time in the geologic records at Sixes River and Bradley Lake when the annual rate of inferred partial CSZ rupture events is less than 0.001. Based on the workshop discussion, most participants would assign higher weight to the onshore geologic observations. Assigning weights of 0.5, 0.25, and 0.25, respectively, to these three branches yields a mean rate is 0.0011 per year, very close to the 0.001 rate recommended in the November 2010 workshop.

Figure P3 shows the effect on a seismic hazard map when the Goldfinger and others (2012) rupture model is used full weight, compared to applying the inputs of the 2008 NSHMs. The peak ground accelerations (PGA) with 2 percent probability of exceedance in fifty years increase substantially along the Oregon and northern California coasts when the Goldfinger and others (2012) model is used. Figure P4 (left panel) shows a hazard map with the Goldfinger and others (2012) model for $M8.0-8.7$ earthquakes applied at half weight, but retaining the hazard from whole-CSZ ruptures. Applying this half weight is equivalent to using the 0.001 rate reported from the onshore geologic data. The hazard values along the southern Oregon and northern California coasts are still significantly higher than those in the 2008 NSHMs (compare maps on left side of figures P3 and P4).

The next node of the logic tree (far right, top) on the segmented model branch is for a northern CSZ rupture, a possibility suggested by Atwater and Griggs (2012), largely from tsunami evidence from Discovery Bay, Washington (Williams and others, 2005). They argue that the additional tsunamis observed at this location that do not correspond in time with Pacific coastal evidence of whole CSZ rupture events may indicate $M8$ ruptures on a northern portion of the CSZ. Others think that these deposits may be from local earthquakes under the Strait of Juan de Fuca or the Georgia Strait. Based on the length of the proposed zone we chose a magnitude of 8.2. One branch is given a recurrence rate of 0.001 per year (Atwater and Griggs, 2012), and the other branch is given a rate of 0. Provisional weights are 0.2 and 0.8, respectively. Note that this possible northern rupture zone is in addition to the more southerly rupture zones specified in Goldfinger and others (2012) that are shown in figure P1 (three panels on right). Figure P4 (right panel) shows a hazard map that uses a northern rupture zone (recurrence rate of 0.001 per year; $M8.2$) along with the southerly rupture zones specified by Goldfinger and others (2012) and whole CSZ ruptures. Note the increase in hazard for northwestern Washington and Vancouver Island when a northern rupture zone is added.

The unsegmented branch of the logic tree entails the use of floating rupture zones. That is, the hazard for each earthquake magnitude is calculated by moving the rupture zone

incrementally along the strike of the CSZ until it reaches the other end. The rate of any particular rupture scenario is simply the total rate for that magnitude divided by the number of rupture zones for that magnitude. We consider two possibilities for the portion of the CSZ to use for the floating ruptures. The first is for ruptures that cover the area from Cape Mendocino to approximately the latitude of the Washington-Oregon border. This is the approximate location of the northernmost cores (Astoria) that Goldfinger and others (2012) report evidence of turbidites from southern CSZ earthquakes. The other option is to have floating ruptures over the entire extent of the CSZ, similar to what was used as a scenario for the 1996, 2002, and 2008 NSHMs (Frankel and others, 1996, 2002; Petersen and others, 2008).

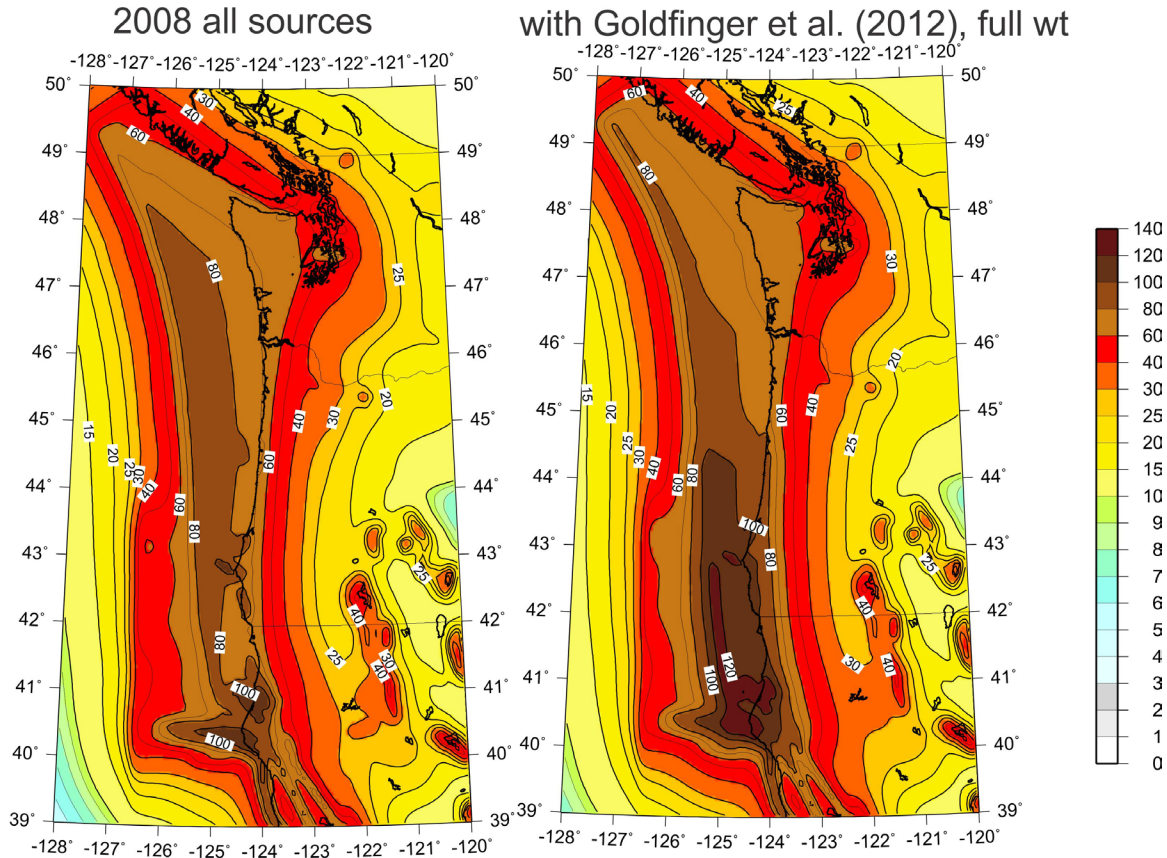


Figure P3. Comparison of seismic hazard maps (PGA in %g with 2% probability of exceedance in 50 years) for (left) the inputs used in the 2008 NSHMs and (right) the Goldfinger and others (2012) model for CSZ great earthquake recurrence. Other hazard sources (gridded shallow and deep seismicity, background zones, and crustal faults) were included in both maps.

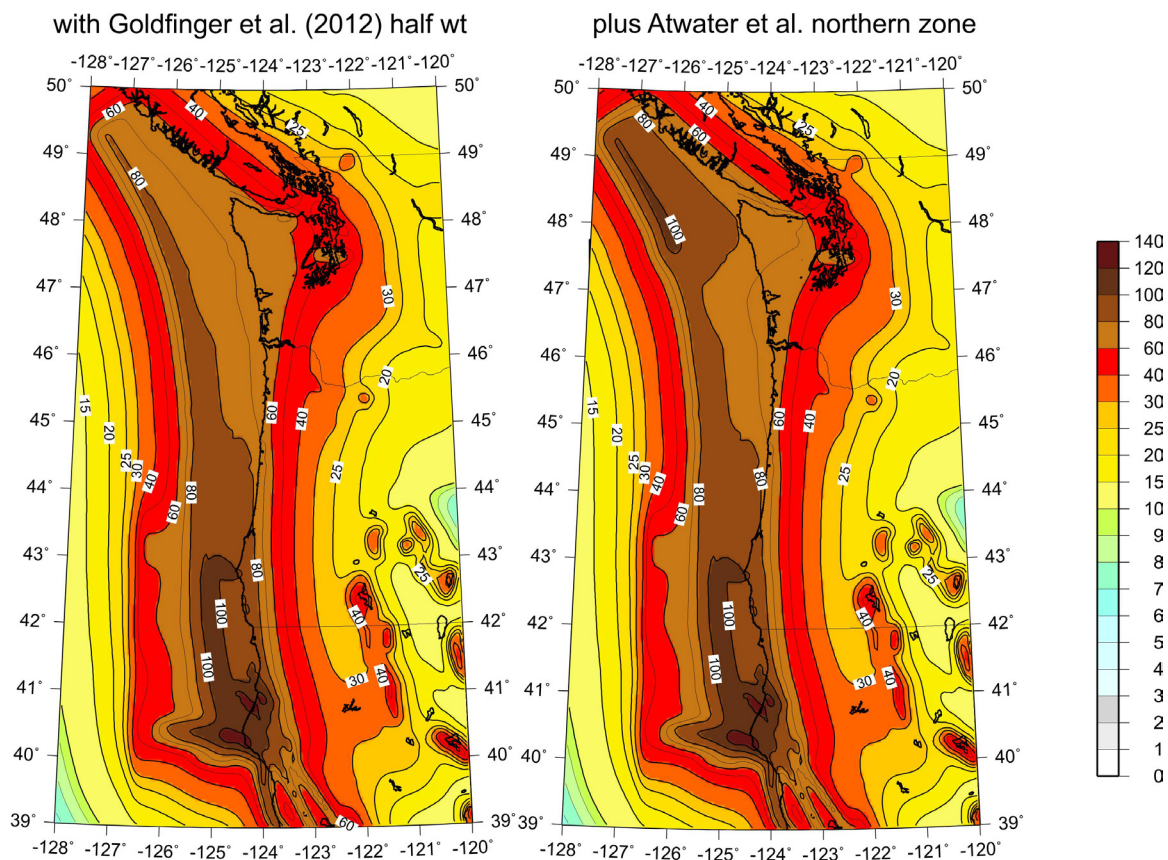


Figure P4. Comparison of seismic hazard maps (2 percent PE in 50 years) for (left) assigning half weight to the $M8.0$ – 8.7 rupture rates from Goldfinger and others (2012) and (right) adding a northern zone ($M8.2$, recurrence rate of 0.001) suggested by Atwater and Griggs (2012). The half weight assigned here for the Goldfinger and others (2012) model essentially corresponds to constraining the total rate of $M8.0$ – 8.7 earthquakes on the southern CSZ to the onshore geologic rate of 0.001. The hazard from whole CSZ rupture events (about $M9.0$) was included in each figure. Other hazard sources (gridded shallow and deep seismicity, background zones, and crustal faults) were included in both maps.

Trial hazard maps for 2 percent probability of exceedance in 50 years indicate that the segmented rupture model of Goldfinger and others (2012) and models with floating ruptures produce very similar hazard maps for onshore locations, if the models are based on the same total rate of $M8.0$ – 8.7 earthquakes. Thus, the mean rate of 0.001 per year is the controlling factor in the hazard maps, rather than the details of the segmentation. The second node of the unsegmented branch describes different models that satisfy the 0.001 mean rate. Here we use a Gutenberg-Richter frequency-magnitude distribution from $M8.0$ – 8.7 . We choose branches with $b=1$ and $b=0$. The $b=1$ branch represents an average global b -value. The $b=0$ branch reflects the unusual nature of the CSZ. Overall, the CSZ does not seem to follow the typical GR relation with b -value of one. Given $M9$ earthquakes with a 500-year recurrence time, we do not see $M7$ earthquakes with 5-year recurrence time, at least over the past 150 years of observations. A b -value of zero implies equal likelihood of having a $M8.0$ or a $M8.7$ earthquake. The 2008 NSHMs essentially used a b -value of about zero for $M8.0$ – 8.7 earthquakes (Petersen and others, 2008). However this scenario represented the hazard from a series of $M8$ earthquakes that fill the CSZ,

as an alternative to whole rupture *M*9 earthquakes. In any case, using a *b*-value of 1 or 0, with an overall rate of *M*8.0–8.7 earthquakes of 0.001 per year, yields very similar seismic hazard maps.

The models that apply floating ruptures over the entire CSZ reflect the idea that there could be an *M*8.0–8.7 earthquake at any location on the CSZ. This is reasonable model, given the uncertainties and the possibility that onshore sites and offshore cores may not have recorded all of the *M*8 earthquakes that occurred on the CSZ. It is problematic to choose a rate for these branches with floating rupture over the entire CSZ. As a provisional solution, we use the same logic tree of rates applied only to the southern ruptures. This choice dilutes the hazard in the southern CSZ (relative to the case with only southern ruptures) to account for the possibility of ruptures in the northern part.

A time-dependent hazard calculation would be straightforward for the whole CSZ rupture scenarios (*M*8.8–9.2 or a series of *M*8 earthquakes), given a 500-year average recurrence time and the time since the 1700 earthquake (Petersen and others, 2002). Calculating time-dependent hazard maps for the *M*8.0–8.7 partial rupture scenarios would be problematic given the variability of the rupture scenarios.

Logic Tree for Down-Dip Edge of Rupture

The location of the down-dip edge of the rupture zones of great Cascadia earthquakes can have substantial effect on the seismic hazard estimates for certain areas. This location is used to determine the closest distance of rupture to a site for the ground-motion prediction equations (GMPEs) used in the seismic hazard calculation. One key issue is how the developers of GMPEs from empirical data identify the edge of a rupture zone. This edge is often determined by slip distributions derived from inversions of strong-motion or teleseismic data. Thus, it corresponds to the location where the coseismic slip is a small fraction of the peak slip on the plate interface during a great earthquake.

During the December 2011 workshop, participants had favorable views of procedures that used modeling of GPS and uplift data to constrain the interseismic locking on the CSZ. They also wanted to use the top of the tremor zone as one model for the location of the down-dip edge of rupture. There have been some suggestions to give low weight to a model with the down-dip edge at the midpoint of the tremor zone. We have not implemented this suggestion at this time.

For the March 2012 workshop, we presented a logic tree that consists of three branches: (1) the average of the 1 cm/yr locking contours from McCaffrey and others (written commun., 2012) and Schmidt and others (written commun., 2012), as determined from modeling GPS and uplift data and applying a down-dip tapering function derived by Kelin Wang, (2) the top of tremor zone based on the compilation of Gomberg and others (2010) and Aaron Wech from http://tunk.ess.washington.edu/map_display/ (Pat McCrory and Luke Blair, written commun., 2012), and (3) the base of the locked zone from Flück and others (1997), based on thermal modeling and uplift data. Figure P5 shows a map with these possibilities.

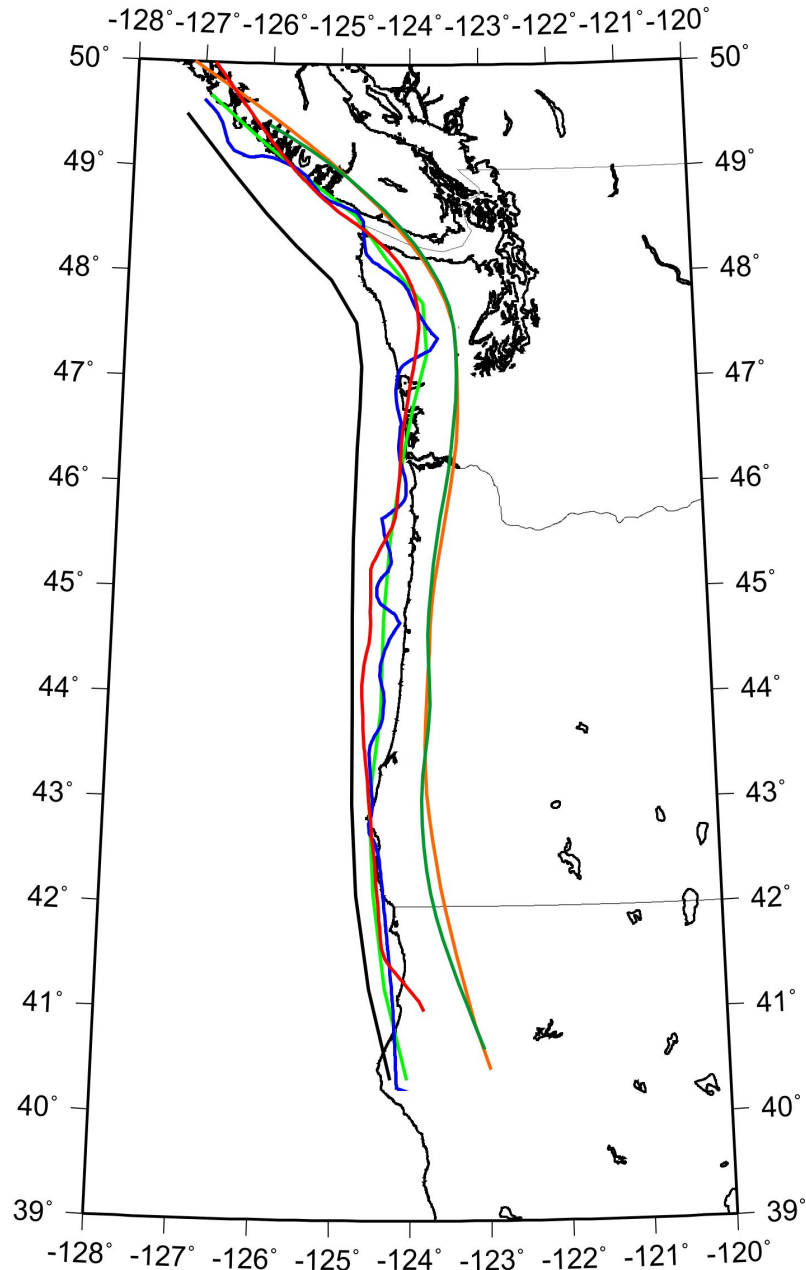


Figure P5. Locations of down-dip edge of rupture used in proposed logic tree. Blue line is the 1 cm/yr locking contour (using tapering function of K. Wang) from McCaffrey and others (written commun., 2012) and red line is the 1 cm/yr contour from Schmidt and others (written commun., 2012). The light green is the approximate average of these two contours. Dark green line is the top of nonvolcanic tremor zone from Gombert and others (2010) and orange is the top of tremor zone from the catalog of A. Wech (written commun., 2011), as determined by Pat McCrory (written commun., 2012). The black line is the base of the fully locked zone from Flück and others (1997), as determined by thermal models and fitting uplift data. We propose to use the midpoint of the updated version of this line and the average of the 1 cm/yr locking contours as the seaward branch in the logic tree.

The March 2012 workshop participants clearly stated that the 1 cm/yr locking contour was an appropriate center of mass of opinion for the location of the down-dip edge. This corresponds to the location on the fault plane with a coupling factor of approximately 0.25. Given the observation that the down-dip part of the rupture zone of the 2011 *M*9.0 Tohoku earthquake that generated significant strong ground motions had a coseismic slip much lower than the peak slip determined for the rupture, workshop participants thought that using the 1 cm/yr locking contour (about 25 percent locking) for the center-of-mass estimate of the down-dip edge was a reasonable strategy.

The March 2012 workshop participants did not have a consensus on the model to use for the most seaward logic tree branch. Participants did express the view that applying the base of the Flück and others (1997) locked zone was too far seaward. As an interim solution, we propose the seaward branch to be located at the midpoint of the base of the locked zone from the updated equivalent of Flück and others (1997) and the 1 cm/yr locking contour from the recent GPS and uplift modeling.

The proposed logic tree for the down-dip edge is shown in figure P6. We assigned provisional weights of 0.5, 0.3, and 0.2, respectively, to the 1 cm/yr locking contour determined from GPS and uplift modeling, the top of non-volcanic tremor, and the midpoint between the base of the fully locked zone and the 1 cm/yr contour.

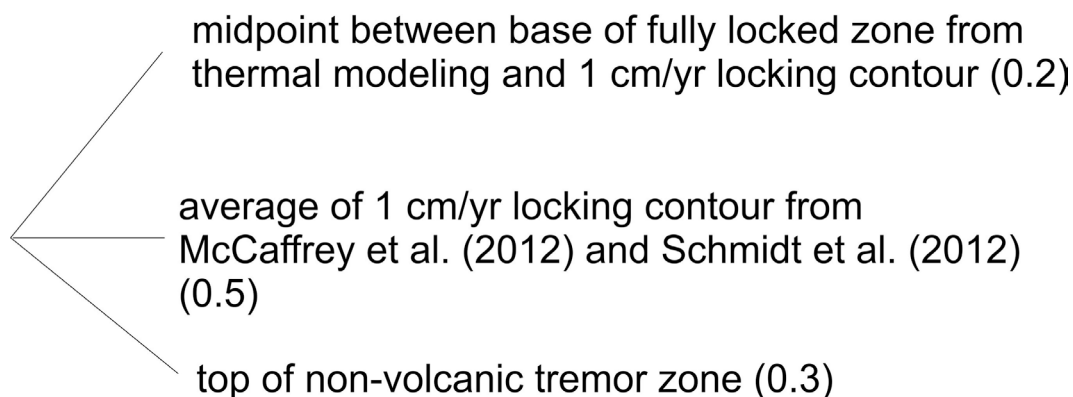


Figure P6. Logic tree for down-dip edge of rupture zones of great Cascadia earthquakes. Initial weight for each branch is given in parentheses.

Acknowledgments

We thank the participants of the three workshops for their comments and suggestions. We especially thank Chris Goldfinger, Brian Atwater, Ray Weldon, Harvey Kelsey, Alan Nelson, Brian Sherrod, and Craig Weaver for their help in this process and for their advice and guidance. Chris Goldfinger hosted the November 2011 workshop. Ray Weldon co-convened the December 2011 workshop. We thank Robert McCaffrey and David Schmidt for supplying the contours of 1 cm/yr locking from their models. Pat McCrory and Luke Blair provided the lines of the top of non-volcanic tremor and contours for the depth to the top of the subducting slab. John Vidale and Brian Atwater reviewed this Appendix. Pat McCrory and Eric Geist provided useful comments.

References

- Adams, J., 1990, Paleoseismicity of the Cascadia subduction zone: evidence from turbidites off the Oregon-Washington margin: *Tectonics*, v. 9, p. 569–583.
- Atwater, B.F., 1987, Evidence for great Holocene earthquakes along the outer coast of Washington state: *Science*, v. 236, p. 942–944.
- Atwater, B.F., 1992, Geologic evidence for earthquakes during the past 2000 years along the Copalis River, southern coastal Washington: *Journal of Geophysical Research*, v. 97, no. B2, p. 1901–1919.
- Atwater, B.F., and Hemphill-Haley, E., 1997, Recurrence intervals for great earthquakes of the past 3,500 years at northeastern Willapa Bay, Washington: U.S. Geological Survey Professional Paper 1576, 108 p., available at <http://pubs.usgs.gov/pp/1576/>.
- Atwater, B.F., and Griggs, G.B., 2012, Deep-sea turbidites as guides to Holocene earthquake history at the Cascadia Subduction Zone—Alternative views for a seismic-hazard workshop: U.S. Geological Survey Open-File Report 2012–1043, 58 p., available at <http://pubs.usgs.gov/of/2012/1043/>.
- Bird, P., and Kagan, Y., 2004, Plate-tectonic analysis of shallow seismicity—Apparent boundary width, beta, corner magnitude, coupled lithosphere thickness, and coupling in seven tectonic settings: *Bulletin of the Seismological Society of America*, v. 94, p. 2380–2399.
- Burgette, R.J., Weldon, R.J., and Schmidt, D.A., 2009, Interseismic uplift rates for western Oregon and along-strike variation in locking on the Cascadia subduction zone, *Journal of Geophysical Research*, v. 114, doi:10.1029/2008JB005679.
- Flück, P., Hyndman, R.D., and Wang, K., 1997, Three-dimensional dislocation model for great earthquakes of the Cascadia subduction zone: *Journal of Geophysical Research*, v. 102, no. B9, p. 539–520, 550, doi:10.1029/97JB01642.
- Frankel, A.D., Mueller, C.S., T. Barnhard, T., Perkins, D.M., Leyendecker, E.V., Dickman, N., Hanson, S., and Hopper, M., 1996, National seismic-hazard maps: documentation June 1996: U.S. Geological Survey Open-File Report 96–532, 110 p.
- Frankel, A.D., Petersen, M.D., Mueller, C.S., Haller, K.M., Wheeler, R.L., Leyendecker, E.V., Wesson, R.L., Harmsen, S.C., Perkins, D.M., and Rukstales, K.S., 2002, Documentation for the 2002 update of the National Seismic-Hazard Maps: U.S. Geological Survey Open-File Report 02–420, p. 33, available at <http://pubs.usgs.gov/of/2002/ofr-02-420/>.
- Frankel, A.D., 2011, Summary of November 2010 meeting to evaluate turbidite data for constraining the recurrence parameters of great Cascadia earthquakes for the update of the national seismic hazard maps: U.S. Geologic Survey Open-File Report 2011–1310, 13 p., available at <http://pubs.usgs.gov/of/2011/1310/>.
- Goldfinger, C., Nelson, C.H., Johnson, J.E., and the shipboard scientific party, 2003, Holocene earthquake records from the Cascadia Subduction Zone and northern San Andreas Fault based on precise dating of offshore turbidites: *Annual Reviews of Earth and Planetary Sciences*, v. 31, p. 555–577.
- Goldfinger, C., Grijalva, K., Burgmann, R., Morey, A.E., Johnson, J.E., Nelson, C.H., Gutiérrez-Pastor, J., Ericsson, A., Karabanov, E., Chaytor, J.D., Patton, J., and Gràcia, E., 2008, Late Holocene rupture of the northern San Andreas Fault and possible stress linkage to the Cascadia Subduction Zone: *Bulletin of the Seismological Society of America*, v. 98, p. 861–889.
- Goldfinger, C., Nelson, C.H., Morey, A., Johnson, J.E., Gutierrez-Pastor, J., Eriksson, A.T., Karabanov, E., Patton, J., Gracia, E., Enkin, R., Dallimore, A., Dunhill, G., and Vallier, T., 2012, Turbidite Event History—Methods and Implications for Holocene Paleoseismicity of the

- Cascadia Subduction Zone: U.S. Geological Survey Professional Paper 1661-F, 332 p., 64 figures.
- Gomberg, J., Bedrosian, B., Bodin, P., Bostock, M., Brudzinski, M., Creager, K., Dragert, H., Egbert, G., Ghosh, A., Henton, J., Houston, H., Kao, H., McCrory, P., Melbourne, T., Peacock, S., Roeloffs, E., Rubinstein, J., Schmidt, D., Trehu, A., Vidale, J., Wang, K., and Wech, A., 2010, Slow-slip phenomena in Cascadia from 2007 and beyond—a review: *Geological Society of America Bulletin*, v. 122, p. 963–978.
- Kelsey, H.M., Witter, R.C., and Hemphill-Haley, E., 2002, Plate-boundary earthquakes and tsunamis of the past 5500 years, Sixes River estuary, southern Oregon: *Geological Society of America Bulletin*, v. 114, p. 298–314.
- Kelsey, H.M., Nelson, A.R., Hemphill-Haley, E., and Witter, R.C., 2005, Tsunami history of an Oregon coastal lake reveals a 4,600 yr record of great earthquakes on the Cascadia subduction zone: *Geological Society of America Bulletin*, v. 117, p. 1009–1032.
- Murotani, S., Miyake, H., and Koketsu, K., 2008, Scaling of characterized slip models for plate-boundary earthquakes: *Earth, Planets, and Space*, v. 60, p. 987–981.
- Nelson, A.R., Shennan, I., and Long, A.J., 1996, Identifying coseismic subsidence in tidal-wetland stratigraphic sequences at the Cascadia subduction zone of western North America: *Journal of Geophysical Research*, v. 101, no. B3, p. 6115–6135.
- Nelson, A.R., Kelsey, H.M., and Witter, R.C., 2006, Great earthquakes of variable magnitude at the Cascadia subduction zone: *Quaternary Research*, v. 65, p. 354–365.
- Pacheco, J.F., Sykes, L.R., and Scholz, C.H., 1993, Nature of seismic coupling along simple plate boundaries of the subduction type: *Journal of Geophysical Research*, v. 98, p. 14133–14159.
- Papazachos, B.C., Scordilis, E.M., Panagiotopoulos, C.B., and Karakaisis, G.F., 2004, Global relations between seismic fault parameters and moment magnitudes of earthquakes, *Bulletin of the Geological Society of Greece*, v. 36, p. 1482–1489.
- Petersen, M., Cramer, C., and Frankel, A., 2002, Simulations of seismic hazard for the Pacific Northwest of the United States from earthquakes associated with the Cascadia subduction zone: *Pure and Applied Geophysics*, v. 159, p. 2147–2168.
- Petersen, M., Frankel, A., Harmsen, S., Mueller, C., Haller, K., Wheeler, R., Wesson, R., Zeng, R.Y., Boyd, O., Perkins, D., Luco, N., Field, E.H., Wills, C., and Rukstales, K., 2008, Documentation for the 2008 Update of the United States National Seismic Hazard Maps: U.S. Geological Survey Open-File Report 2008-1128, 61 p.
- Satake, K., Shimazaki, K., Tsuji, Y., and Ueda, K., 1996, Time and size of a giant earthquake in Cascadia inferred from Japanese tsunami record of January 1700: *Nature*, v. 379, p. 246–249.
- Satake, K., Wang, K., and Atwater, B.F., 2003, Fault slip and seismic moment of the 1700 Cascadia earthquake inferred from Japanese tsunami descriptions: *Journal of Geophysical Research*, v. 108, no. B11, p. 2535, doi:10.1029/2003JB02521.
- Strasser, E.O., Arango, M.C., and Bommer, J.J., 2010, Scaling of the source dimensions of interface and intraslab subduction-zone earthquakes with moment magnitude, *Seismological Research Letters*, v. 81, p. 951–950.
- Toro, G.R., and Silva, W.J., 2001, Scenario earthquakes for Saint Louis, MO, and Memphis, TN, and seismic hazard maps for the central United States region including the effect of site condition: Technical report to U.S. Geological Survey, Reston, Virginia, under Contract 1434-HQ-97-GR02981, <http://www.riskeng.com/publications/>.

Williams, H.F.L., Hutchinson, I., and Nelson, A.R., 2005, Multiple sources for late-Holocene tsunamis at Discovery Bay, Washington state, USA: *The Holocene*, v. 15, no. 1, p. 60–73, doi:10.1191/0956683605hl784rp.

Wilson, D.S., 2002, The Juan de Fuca plate and slab—Isochron structure and Cenozoic plate motions: U.S. Geological Survey Open-File Report 02-328, p. 9–12.

Witter, R.C., Kelsey, H.M., and Hemphill-Haley, E., 2003, Great Cascadia earthquakes and tsunamis of the past 6700 years, Coquille River estuary, southern coastal Oregon: *Geological Society of America Bulletin*, v. 115, p. 1289–1306.